Biogeochemistry (2025) 168:50
https://doi.org/10.1007/s10533-025-01240-9

The colloidal fraction of dissolved organic matter extracted from a forest soil persists microbial decomposition

Erika Andersson · Marloes Groeneveld · Lars Tranvik · Anders Tunlid · Per Persson · Ulf Olsson

Received: 27 January 2025 / Accepted: 30 April 2025
© The Author(s) 2025

Abstract We have investigated the bacterial decomposition of dissolved organic matter (DOM) extracted from the organic layer of a boreal forest soil and filtered at a pore size of 0.2 µm. This DOM source has previously been extensively characterized and contains approximately equal amounts by carbon of a colloidal fraction, mainly composed of carbohydrates, and a fraction of molecularly dissolved DOM. Here, extracts were inoculated with soil bacteria and the decomposition of DOM was followed over a period of 2 months, during which it was analyzed with scattering methods and ^{1}H NMR, and by measuring the concentration of total organic carbon. A comparison was also made with dialyzed extract. Results showed that while the bacteria fully decomposed the molecular fraction within approximately two weeks, the colloidal fraction was stable with no visible decomposition within the 2 months. The results indicate the importance of distinguishing small molecules from colloidal aggregates in decomposition studies, and demonstrate the usefulness of combining scattering methods with ^{1}H NMR for this purpose.

Keywords Dissolved organic matter · Organic colloids · Small angle scattering · ^{1}H NMR · Decomposition · Soil

Responsible Editor: Jacques C. Finlay.

Supplementary Information The online version contains supplementary material available at https://doi.org/10.1007/s10533-025-01240-9.

E. Andersson (✉) · M. Groeneveld · L. Tranvik
Department of Ecology and Genetics, Limnology, Uppsala University, Uppsala, Sweden
e-mail: erika.andersson@ebc.uu.se

E. Andersson · U. Olsson
Department of Chemistry, Division of Physical Chemistry, Lund University, Lund, Sweden

M. Groeneveld
Department of Soil and Environment, SLU, Uppsala, Sweden

A. Tunlid · P. Persson
Department of Biology, Lund University, Lund, Sweden

P. Persson
Centre for Environmental and Climate Science, Faculty of Science, Lund University, Lund, Sweden

Introduction

Dissolved organic matter (DOM) is considered to be bioavailable and mobile in soils (e.g., Davidson et al. 1987; Qualls and Haines 1992; Marschner and Kalbitz 2003), and is hence important for the cycling of carbon and nutrients, both within terrestrial ecosystems and between ecosystems (e.g., Cleveland et al. 2004; Bolan et al. 2011). In inland waters and oceans, DOM constitutes the major organic carbon pool (Søndergaard and Middelboe 1995; Schlesinger 2020; Catalá et al. 2021). DOM is generally

Published online: 16 May 2025

operationally defined as the organic matter that is not retained by filtration, commonly using pore sizes of 0.45 or 0.2 µm (Herbert and Bertsch 1995; Findlay and Parr 2017). Hence, in addition to dissolved molecules, DOM can also comprise organic particles or aggregates of a size up to the filter pore size used. This kind of suspended, non-crystalline particles in the size range of 1 nm to 1 µm are generally referred to as colloids (Evans and Wennerström 1999).

Experimental studies have found different decomposition rates for different components of DOM (e.g., Kalbitz et al. 2003a; Marschner and Kalbitz 2003; Bowen et al. 2009; Koehler et al. 2012), ranging in half-life from minutes or hours to months, and a fraction that does not decompose at the experimental time scales. This recalcitrant fraction is particularly interesting from the point of view of carbon sequestration, and its size varies between different studied systems (Qualls and Haines 1992; Kalbitz et al. 2003a; Cleveland et al. 2004; Andreasson et al. 2009; Bowen et al. 2009). Several different factors may explain the variable biodegradability of DOM (Marschner and Kalbitz 2003; Kothawala et al. 2021; Berggren et al. 2022). Factors often suggested include composition (Kalbitz et al. 2003a, b; Marschner and Kalbitz 2003; Kiikkilä et al. 2006; Kellerman et al. 2015; Grasset et al. 2023), molecular weight distribution (Tranvik 1990; Amon and Benner 1994, 1996) and protection by adsorption to mineral surfaces or formation of aggregates (Marschner and Kalbitz 2003; Kalbitz et al. 2005; Mueller et al. 2012; Lehmann and Kleber 2015). While the role of mineral particles in protecting soil organic matter from microbial decomposition has been well studied (Kleber et al. 2015), less is known on the impacts of colloidal organic aggregates. Colloidal assembly has been suggested to constrain DOM biodegradability (Dreves et al. 2007; Yan et al. 2018; Lehmann et al. 2021; Meklesh et al. 2022), however, direct studies of how colloidal and non-colloidal DOM change during exposure to microbial decomposition are few.

Recently, we presented a multi-technique approach combining spectroscopic and scattering methods to characterize the chemical and colloidal properties of DOM (Meklesh et al. 2022; Andersson et al. 2023a, b). The chemical composition of the DOM was analyzed using ^{1}H NMR. Though NMR spectroscopy cannot give the same detailed molecular characterization of DOM as high-resolution mass spectrometry, NMR can provide a better representation of the bulk composition since this technique is not hampered by the selectivity of the ionization process in mass spectrometry (Nebbioso and Piccolo 2013). Scattering techniques can provide information on the size, physical structure, concentration, and charge of colloids, and they are widely applied in studies of soft matter (Glatter 2018). The scattering methods used in our studies will detect colloids spanning the size range of ca 2–200 nm (Meklesh et al. 2022; Andersson et al. 2023a), which is consistent with the pore size (0.2 µm) of the membrane filters used for isolating the DOM. X-ray scattering techniques can probe the smaller colloidal sizes, while scattering techniques using visible light cover the larger size range.

Applying these methods for characterizing DOM extracted by water from the soil of a boreal forest in southern Sweden showed that the DOM can roughly be divided into two fractions: molecularly dissolved DOM, referred to here as "molecular DOM", and dispersed colloidal particles, with sizes up to the filter pore size, referred to as "colloidal DOM". There is no strict size boundary between these two fractions, however, we apply an operational separation based on dialysis (Meklesh et al. 2022) and the inherent size bias of the NMR and scattering methods used. The molecular DOM is readily detected in a solution ^{1}H NMR spectrum as it gives rise to narrow sharp lines. The colloidal DOM, on the other hand, gives rise to broad ^{1}H NMR lines, due to slow rotational diffusion of the large aggregates (Wennerström and Ulmius 1976; Ulmius and Wennerström 1977; Olsson et al. 1986; Fernández and Wider 2006). Instead, in scattering experiments, there is a strong bias towards larger objects (Glatter 2018) and essentially only the colloidal DOM is "visible". We have previously found this colloidal DOM to be dominated by carbohydrates (Andersson et al. 2023b), but also molecular DOM to contain a significant amount of carbohydrate molecules (Meklesh et al. 2022; Andersson et al. 2023a).

In this study, we take advantage of a well-characterized DOM starting material and follow its bacterial decomposition during two months of incubation by time-resolved scattering, ^{1}H NMR, and organic carbon concentration. We test the hypothesis that the decomposition kinetics is significantly different between molecular and colloidal DOM, and our experimental toolbox allows us to explicitly compare

the decomposition rates, and hence the bioavailability, of these two fractions.

Materials and methods

Soil sampling

Soil from the whole organic layer of a first-generation Norway spruce forest was collected in September 2021 for the incubation experiments, and in April 2024 for the dialysis experiment. The forest was located at Tönnersjöheden experimental forest in southwest Sweden (56°41′6.0″N, 13°6′32.0″E) and planted in 1957. For description of the sampling site, see Škerlep et al. (2022). The soil was sieved (2 mm) to remove larger organic and inorganic particles, kept field moist, and stored dark in sealed plastic bags at 4 °C. The 2021 soil was stored for 6 months before extraction for the long incubation experiment, and for 12 months before extraction for the short time incubation. The 2024 soil was stored for 5 days before extraction. The results presented below do not indicate any differences in the chemical composition or the colloidal properties of the extracted DOM due to soil storage time.

DOM extraction

DOM was extracted according to the method described in our previous work (Andersson et al. 2023a). In short, soil and Milli-Q water (resistivity 18.2 MΩ.cm, Merck AG, Darmstadt, Germany) were mixed in a ratio of 1:5 w/v and stirred on a magnetic stirring plate at 4 °C for 24 h. The soil suspension was pressed through a nylon mesh (150 µm pores, Safar, Heiden, Switzerland), centrifuged at 1700 g for 5 min, and sequentially filtered through glass microfiber filters (GF/D, GF/A, GF/F, Whatman, UK). Finally, the extract was filtered through a sterile PES membrane filter with 0.2 µm pore size (Sarstedt AG \& Co. KG, Nümbrecht, Germany) into sterile polypropylene bottles. The extracts were stored dark at 4 °C (1–10 days) prior to incubation or dialysis.

Inoculation and incubation

An inoculum was obtained by shaking 1.2 g of the same type of soil as used for DOM extraction with 60 ml Milli-Q water for 10 min by hand in a glass bottle. The suspension was filtered through glass microfiber filters (GF/D, GF/A, Whatman, UK) down to 1.6 µm pore size and stored dark at 4 °C for one week before inoculation. Elemental analysis of the inoculum is found in Table S1. We refer to the microbes of the inoculum as bacteria based on the cut-off size used, although it may include archaea, viruses, and some predators (bacterivorous protists).

DOM extracts were inoculated with 1% v/v of the inoculum. Triplicates of ca. 45 ml inoculated DOM were transferred to 50 ml polypropylene tubes and incubated dark at 21 ± 2 °C. The tubes were gently shaken and aerated approximately every second day to supply oxygen. Aliquots for chemical analyses were taken out after 8, 14, 28 and 56 days (8, 14, 27 and 55 days for TOC/TN), and for scattering after 14, 28 and 56 days. Triplicates of non-inoculated DOM were incubated in separate tubes for each analyses time point as controls (ca. 10 ml DOM in 15 ml polypropylene tubes). These were not aerated, to avoid contamination during the incubation period and since no significant oxygen consumption was expected.

Dialysis

A separate batch of DOM extract was dialyzed at a molecular weight cut-off of 3.5 kDa using cellulose dialysis membranes (Spectra/Por®, Spectrum Laboratories Inc., California, USA). The membrane was soaked in Milli-Q water for at least 30 min and rinsed before filling with the sample. The dialysis was performed for 7 days at 4 °C under stirring, with a sample:Milli-Q ratio of ca 25, and the Milli-Q exchanged approximately every 24 h. The retentate was collected for further analysis.

Chemical analysis

Concentrations of total organic carbon (TOC) and total nitrogen (TN) were analyzed using a TOC-VCPH equipped with a TNM-1 unit (Shimadzu Corp., Kyoto, Japan). Calibration for TOC analysis was performed with potassium hydrogen phthalate (KHP) and ethylenediaminetetraacetic acid (EDTA) was used as a secondary standard to check the calibration curve. Calibration for TN was performed with KNO_3. The aliquots taken out for TOC and TN analysis at each time point during the incubation study

were frozen and stored (no other samples were frozen). Freezing was done to stop the decomposition, and they were stored so that all samples could be analyzed for TOC and TN in a single day.

Phosphorus (P) and iron (Fe) concentrations were measured in the original extracts and inoculum (Table S1) by Inductively Coupled Plasma Optical Emission Spectrometry (ICP-OES) on an Optima 8300 (PerkinElmer, Inc., Waltham, USA).

pH was measured on day 1, 8, 15, 29 and 58 (Table S2) using a Ross Sure-flow Semi Micro electrode (Thermo scientific, USA) connected to a PHM210 MeterLab pH meter (Radiometer Copenhagen, Brønshøj, Denmark).

High resolution ^{1}H NMR spectra were recorded on a Bruker Avance III HD 500.17 MHz spectrometer (Bruker, Billerica, MA, USA) equipped with a 5 mm broadband probe, at 25 °C. Excitation sculpting (Hwang and Shaka 1995) was used for suppression of the large water peak. For details on measurement settings see Meklesh et al. (2022). Spectra were processed with a Lorentzian line broadening factor of 2 Hz and zero- and first-order phase corrected in TopSpin 4.0.7 software (Bruker, Billerica, MA, USA). At each time point, one sample was also measured after re-filtering 0.2 µm, to track any influence from bacteria on the NMR signal. However, spectra from filtered and non-filtered samples were very similar (Fig. S1).

A rough separation into different chemical classes was performed by dividing the ^{1}H NMR spectra into 5 different regions, R1-R5 (Meklesh et al. 2022; Andersson et al. 2023a). These were: R1 (0.6–1.65 ppm), aliphatic components; R2 (1.65–2.2 ppm), acids; R3 (2.2–3.0 ppm), esters; R4 (3.0–4.3 ppm), carbohydrates; R5 (6.0–9.0 ppm) aromatics. See further explanation and details in the supplementary information (Text S1 and Fig. S2). Total NMR intensity (NMR_{int}) was quantified as the integrated area in the region 0.6–4.3 ppm + 6.0–9.0 ppm. The relative intensity was analyzed as intensity of one region divided by NMR_{int} for that spectrum.

Dynamic light scattering and ζ-potential

Dynamic light scattering (DLS) and determination of ζ-potential were performed at 25 °C on a Zetasizer Ultra at day 1, and a Zetasizer Nano ZS instrument (Malvern Instruments, Ltd., Worcestershire, UK) at day 14, 28 and 56 of the incubation study. Inoculated samples were re-filtered 0.2 µm prior to measurements. The Nano ZS instrument was used in the dialysis study. The DLS experiments were performed at a scattering angle of 173° and the ζ-potential experiments at 13°. The mean hydrodynamic radius ($\langle R_H \rangle$), polydispersity index (PDI), and ζ-potential were calculated for each sample from three consecutive measurements as described in Meklesh et al. (2022), using the Zetasizer software (Malvern Instruments, Ltd., Worcestershire, UK). From these, mean values with standard deviations were calculated for inoculated and control samples respectively.

Static scattering

Measurements of small angle X-ray scattering (SAXS) and static light scattering (SLS, only on day 0 and 56) were performed as described in more detail in Andersson et al. (2023a), to obtain the scattered intensity $I(q)$. Here q is the scattering vector given by $q = \frac{4\pi n}{\lambda} sin\left(\frac{\theta}{2}\right)$, where n is the refractive index of the sample, λ is the radiation wavelength, and θ is the scattering angle. For SAXS, $n = 1$ and $\lambda = 1.54$ Å. In SLS, $n = 1.33$ and the laser had a wavelength $\lambda = 633$ nm.

SAXS experiments were performed at 25 °C under vacuum, using a laboratory-based GANESHA instrument (SAXSLAB ApS, Skovlunde, Denmark). The two-dimensional (2D) SAXS patterns were radially averaged using SAXSGui software, and background, including solvent scattering, was subtracted. Water was used as a standard for absolute scaling of the data.

SLS experiments were performed at 25 °C on an ALV/DLS/SLS-5022F compact goniometer system (ALVGmbH, Langen, Germany), equipped with a 22 mW HeNe laser. A software-controlled attenuator varied the laser intensity. Cis decahydronaphthalene was used for refractive index matching of the sample cells. SLS samples were diluted 50–100 times with Milli-Q water and inoculated samples were re-filtered 0.2 µm before measurements to avoid large intensity spikes from bacteria. Solvent scattering was subtracted and toluene was used as a standard for absolute scaling of the data (Andersson et al. 2023a).

The scattered intensity $I(q)$ from a dispersion of colloidal particles can be written as

$I(q) = cKMP(q)$ where c (mass per volume) is the particle concentration, M is the particle molar mass and where K involves the scattering contrast. In the case of X-rays (SAXS) $K = K_{SAXS} = \frac{\Delta\rho^2}{\delta^2 N_A}$. Here, $\Delta\rho$ is the scattering length density difference between particle and solvent, δ is the particle mass density and N_A is Avogadro's number. In the case of (visible) light scattering, SLS, we have $K = K_{SLS} = \frac{4n^2\pi^2}{\lambda^4 N_A}\left(\frac{dn}{dc}\right)^2$ where dn/dc is the refractive index increment. For a binary system, a single kind of particles in a solvent, SLS and SAXS data can be plotted together on the same scale by e.g. transforming the SLS data to SAXS contrast, by multiplying the SLS $I(q)$ by K_{SAXS}/K_{SLS} as was done here. The colloidal DOM has been found to consist mainly of carbohydrates (Meklesh et al. 2022; Andersson et al. 2023a, b). Following these works, we assume the colloids to be made up of hemicellulose having an X-ray scattering density of $\rho = 13.5 \cdot 10^{10}$ cm^{-2}, and a mass density of δ=1.5 g/ml. The X-ray scattering density of water $\rho_w = 9.5 \cdot 10^{10}$ cm^{-2}, giving $\Delta\rho = 4 \cdot 10^{10}$ cm^{-2}. For SLS we assumed dn/dc=0.144 cm^3/g (Andersson et al. 2023a). With these values for the SAXS and SLS contrast, respectively, the SLS data were converted to SAXS contrast, with good agreement between the two data sets. Finally, $P(q)$ is the normalized $(P(0)=1)$ particle form factor that carries information on the particle size and shape. We note that the scattering is strongly biased towards larger particles, and thus reports mainly on the colloidal fraction of DOM.

Results and discussion

The DOM consists of various dissolved molecules (molecular DOM) coexisting with a colloidal fraction (colloidal DOM). In Fig. 1, we present ^{1}H NMR spectra of the initial DOM before any bacterial decomposition (time point $t=0$, Fig. 1a, b) or dialysis (Fig. 1c). The NMR spectra in Fig. 1a were obtained from the same incubated material as the scattering patterns in Fig. 2. The NMR spectra in Fig. 1b were recorded in a second short incubation, using a new batch of extract, to have data with a higher time resolution. The dialysis experiments (Fig. 1c) were performed using a third extraction batch. The NMR spectra at $t=0$, as well as the elemental concentrations, ζ-potential and DLS results (Table S1), were very similar to what we have reported previously for DOM from this boreal forest soil (Meklesh et al. 2022; Andersson et al. 2023a).

The NMR spectrum consists of a number of sharp peaks, resulting from the molecular DOM, on top of some broad peaks resulting from the colloidal DOM (Wennerström and Ulmius 1976; Ulmius and Wennerström 1977; Olsson et al. 1986; Fernández and Wider 2006). The broad ^{1}H resonances from the colloidal DOM are somewhat "masked" by the many sharp peaks, but Meklesh et al. (2022) used dialysis to confirm the broad peaks from the colloidal fraction. See also the discussion on the ^{1}H NMR spectrum features in Text S2. The chemical shift (given in ppm) depends on the local environment of the protons. The relatively higher integral of R4 compared to other regions (Fig. 1 and Fig. S2) suggests that carbohydrates were a major component of the DOM. This is consistent with previous observations (Meklesh et al. 2022; Andersson et al. 2023a), where it was also confirmed by chemical analysis (Meklesh et al. 2022).

The NMR intensity decreased rapidly during the first days of incubation (Fig. 1a, b) and then reached a steady state after ca. 8 days. After day 8, the spectrum remained essentially constant until the last time point at 56 days. Narrow peaks disappeared in the first few days, and after day 8, the spectrum consisted only of broad resonances. The highest intensity at the end of incubation was still found in the carbohydrate region R4. However, a significant intensity was also seen in R1 (aliphatic) where two different peaks appeared, most likely representing –CH2– (1.2 ppm) and –CH3 (0.8 ppm) groups, possibly originating from waxes. In addition to the rough separation of chemical classes (R1–R5), we can also identify a few specific compounds in the spectra, such as acetic acid (singlet 1.9 ppm) (Whitty et al. 2019). However, this peak was no longer visible at the end of incubation. The rapid loss of sharp peaks together with the persistence of broader peaks throughout the incubation implies that the molecular DOM was readily decomposed, for all types of functional groups, while the colloidal fraction was not.

This conclusion is supported by the dialysis results, in which we also observe the removal of sharp peaks. The ^{1}H NMR spectra from dialyzed and incubated DOM overlap, apart from a slightly higher intensity in R1-2 in the incubated DOM

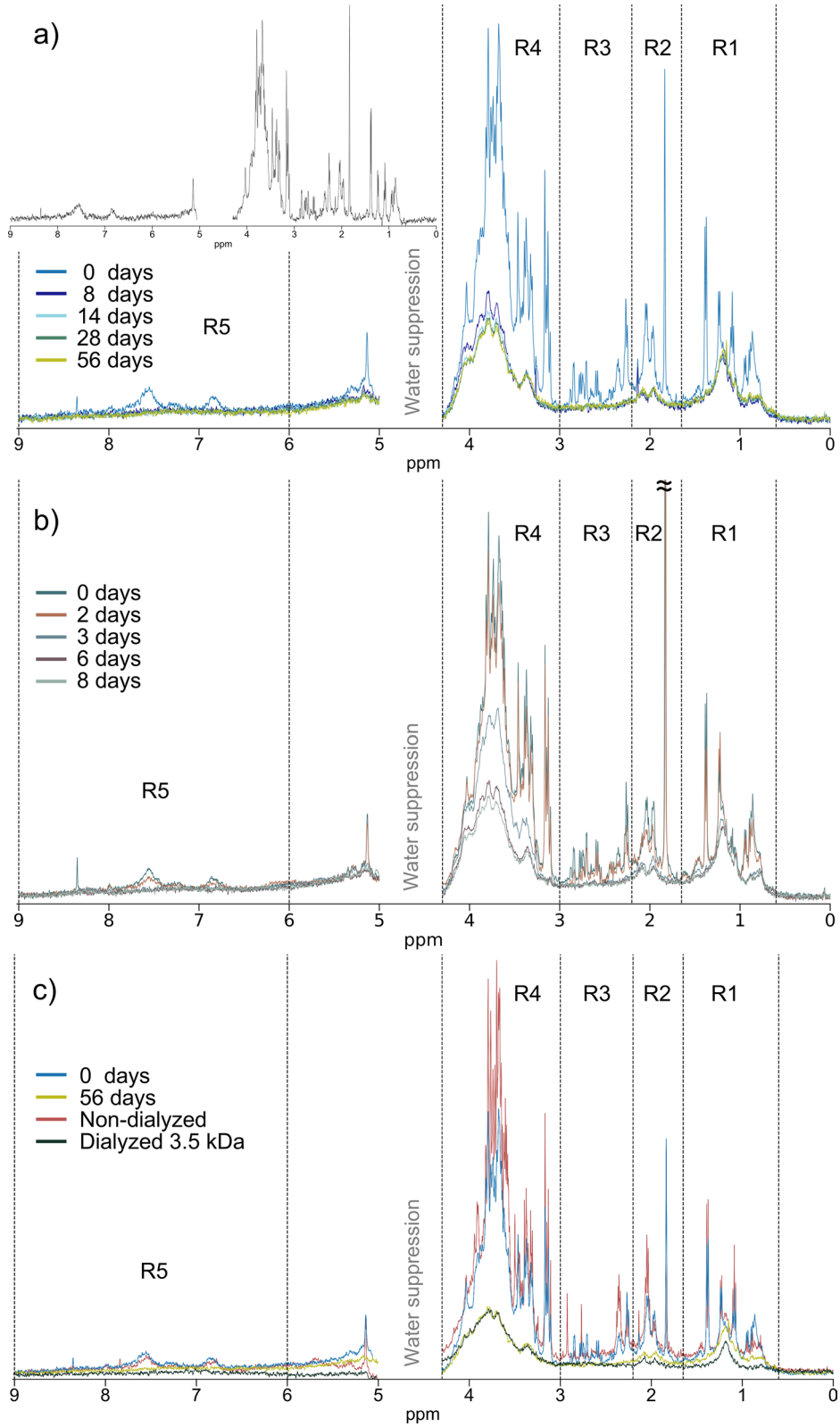
a)
R4
R3
R2
R1
0 days
8 days
14 days
28 days
56 days
R5
Water suppression
ppm
b)
R4
R3
R2
R1
0 days
2 days
3 days
6 days
8 days
R5
Water suppression
ppm
c)
R4
R3
R2
R1
0 days
56 days
Non-dialyzed
Dialyzed 3.5 kDa
R5
Water suppression
ppm

◂**Fig. 1** **a** ^{1}H NMR spectra of samples taken at different time points during incubation. As the triplicates were very similar, only one spectrum from each time point is shown. The inset shows the difference between the spectra from day 0 and day 56, representing removed material. **b** ^{1}H NMR spectra of samples from a different extraction batch used in a second short incubation study to get higher initial temporal resolution. **c** ^{1}H NMR spectra of samples from a third extraction batch before and after dialysis using a 3.5 kDa cut-off membrane, compared with the data from day 0 and 56 of incubation shown in **a**. In all panels, R1-R5 indicates our separation of chemical classes. Peaks marked with ≈ are cut for clarity

(Fig. 1c). This similarity strongly suggests that the signal observed after the incubation originates from the colloidal fraction.

The combined SAXS and SLS scattering profile (Fig. 2) shows the presence of colloidal aggregates with sizes of the order of 100 nm. Again consistent with previous observations (Meklesh et al. 2022; Andersson et al. 2023a), the scattering pattern is well described by a model *P(q)* of mass fractal particles, here having a radius of gyration $R_g = 60$ nm and fractal dimension $d = 2.8$. The model is described in more detail in Text S3.

In contrast to the NMR intensity, the SLS/SAXS intensity did not change during the incubation period. The scattering pattern obtained at $t = 56$ days was essentially the same as the initial one at $t = 0$ (Fig. 2). This is further highlighted in the inset of Fig. 2, showing the SLS data on a linear scale where also small intensity changes would be visible. There were also no changes observed in $\langle R_H \rangle$ from DLS (Table S3). This is consistent with the NMR data and confirms that no distinguishable decomposition of the colloidal fraction occurred during the 56 days.

The initial rapid loss of NMR intensity observed during incubation was consistent with the change in TOC concentration, i.e., the relative loss rates of TOC (for concentrations see Table S2) and NMR_{int} were similar (Fig. 3). They both leveled off and reached a steady state of ca. 50% after approximately 8 days. The TOC concentration and NMR_{int} of the control samples that were not inoculated did not change during the first 4 weeks of incubation (Fig. 3, spectra in Fig. S3). This supports the interpretation that the decrease observed in the inoculated samples was due to bacterial decomposition. However, a 20% decrease was observed after 56 days, indicating that the control samples were not sterile. No reduction was observed in the SLS/SAXS intensity of the controls (Fig. S4).

Dialysis resulted in a total decrease in TOC concentration (Table S2) and NMR_{int} of ca. 60%. This provides a quantification of the colloidal fraction for this kind of extract, and the similarity between loss of non-colloidal matter by dialysis and by incubation with microorganisms, further supports the persistent nature of the colloids.

The data strongly indicate two fractions of DOM that are differentially available for bacterial decomposition, i.e., a labile fraction, f_l, composed of dissolved molecules, and an essentially stable fraction, $f_s = 1\text{-}f_l$, corresponding to the colloidal fraction. This can be integrated into a simple model with one exponentially decaying and one recalcitrant fraction

$$\frac{A(t)}{A_0} = f_l e^{-kt} + \left(1 - f_l\right) \quad (1)$$

where *A(t)* is the time dependence of either TOC or the NMR integral, and k is the corresponding decay rate. Based on the data in Fig. 3, we obtain for TOC $f_l = 50 \pm 6\%$ and $k = 0.2 \pm 0.1$ days^{-1}, and for the NMR integral $f_l = 56 \pm 4\%$ and $k = 0.3 \pm 0.1$ days^{-1}.

To summarize, the soil-extracted DOM of the present study was a mixture of approximately 50% molecular DOM and 50% colloidal DOM. We found that the molecular fraction of DOM was readily decomposed upon inoculation. After approximately 2 weeks, all dissolved molecules had been decomposed, as viewed by ^{1}H NMR. The colloidal fraction, on the other hand, was persistent. Essentially no decomposition of this material was observed for up to two months of incubation. This is a striking result, in particular considering that the colloidal DOM is dominated by carbohydrates (Andersson et al. 2023b). The results presented strongly support our hypothesis that the decomposition kinetics of molecular and colloidal DOM differ. It is interesting to compare our results with the recent findings of Gentile et al. (2024), who investigated the decomposition of a similar DOM by two specific fungi, the saprotrophic fungus *Gloeophyllum*, and the ectomycorrhizal fungus *Paxillus involutus*. Also with those decomposers, it was observed that molecular DOM was relatively rapidly decomposed, while the colloidal fraction was significantly more stable, although with some differences between the two fungi.

Previous studies of loss of organic carbon from soil solution in similar batch cultures show a large range

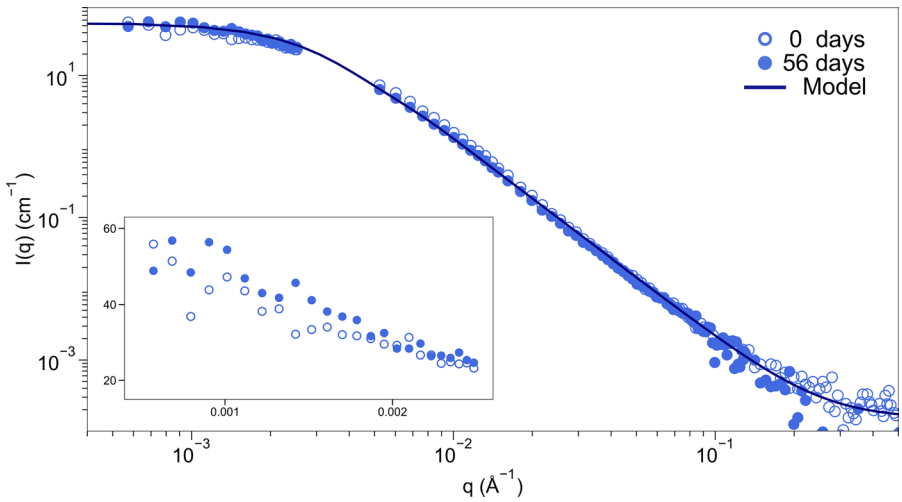

Fig. 2 Scattering patterns from the start and end time of incubation. The solid line is a model calculation representing mass fractal particles, described in Text S3. The inset shows the SLS data on a linear scale. Replicates and controls overlap with the scattering data shown

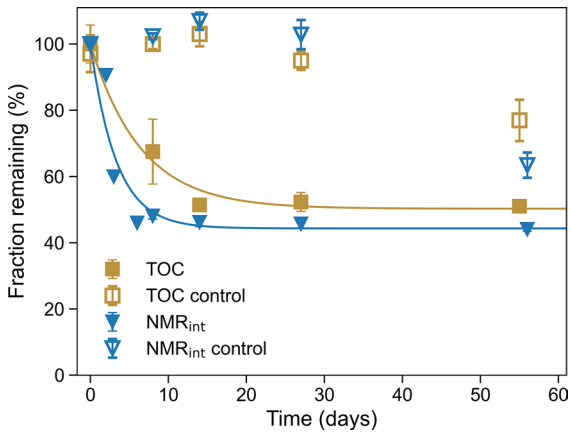

Fig. 3 Remaining fraction of TOC and total NMR intensity (NMR_{int}) (%), as a function of incubation time for inoculated samples and controls. Data points represent mean values ± one standard deviation from triplicates where applicable. There were no replicates in the short time NMR incubation study. Lines represent fitted exponential decays according to Eq. 1

of microbial mineralization. The degradable fraction of DOC leaching fresh litter has been estimated to be between 33 and 95% (Don and Kalbitz 2005). DOM in soils has been found to have a degradable fraction ranging from just a few percent up to 65% (Liu et al. 2021). A review of batch culture assessments of DOC degradability in aquatic environments (Søndergaard and Middelboe 1995), showed median labile fractions in lakes, rivers, and marine waters of 12, 25, and 14%, respectively. The estimated degradable fraction depends strongly on experimental conditions such as length of incubation, temperature, and inorganic nutrients (Marschner and Kalbitz 2003). Moreover, the organic matter constitutes a range of compounds of different degradability, resulting in a reactive continuum rather than discrete fractions that are either degradable or refractory (Koehler et al. 2012).

It is well established that different fractions of DOM may show widely different decomposition kinetics. Several suggestions exist in the literature for this difference, including intrinsic molecular properties (Kothawala et al. 2021), and extrinsic factors such as molecular adsorption to mineral surfaces (Schmidt et al. 2011). Only a minor amount of Fe was detected in the DOM extracts studied here, ≈1 mg/l to be compared with TOC≈100 mg/l (Table S1), as the soil was sampled from the organic layer. The specific Fe species are unknown; however, X-ray absorption spectroscopy (XAS) of boreal soils and waters has demonstrated that Fe can exist in various forms, including Fe(hydr)oxides and Fe complexed with organic material (Sundman et al. 2014). Two recent studies have investigated the possible association of DOM, from soil in the same area as sampled in this study, with ferrihydrite (Gentile et al. 2018) and hematite (Andersson et al. 2023b), respectively. The experiments revealed that molecular DOM promoted aggregation of the mineral particles, whereas no interactions were observed between the mineral particles and colloidal DOM. Collectively, this suggests that the colloidal fraction in the present study was not protected from decomposition due to adsorption to iron-oxide mineral particles.

Previous studies of how aggregation of molecules affects recalcitrance of DOM address a broad range of environments but also reflect different size windows. Larger aggregate sizes in inland waters have been demonstrated to be more reactive than DOM (Attermeyer et al. 2018), and coagulation of colloids on bubble surfaces in the ocean may enhance microbial degradation (Kepkay and Johnson 1989; Kepkay 1994). Moreover, DOM in marine and fresh waters has been shown to increase in degradability with increasing molecular weight within a size spectrum reaching the lower end (≈10 kDa, or ≈1 nm radius) of the colloidal size spectrum studied here (Tranvik 1990; Amon and Benner 1994, 1996). We still lack consistent studies and a broader understanding of how aggregation and aggregate size affect degradability, particularly in the colloidal size range.

Conclusions

To conclude, our results support our hypothesis and show that colloids play a major role in the persistence of DOM, in a soil extract. It remains to be addressed to what extent our finding applies to DOM in other environments, including pelagic waters of lakes and oceans, and with other decomposer types. However, our results suggest that the physical difference between molecular and colloidal fractions could be an important, but hitherto mostly overlooked, aspect of the central question of what makes organic matter either reactive or persistent in different environments and across different time scales. This study further highlights the potential of scattering methods and ^{1}H NMR for the investigation of the role of colloids in the reactivity of organic matter.

Author contributions All authors contributed to the study conception and design. Material preparation, data collection and analysis were performed by Erika Andersson and Marloes Groeneveld. The first draft of the manuscript was written by Erika Andersson and all authors commented on previous versions of the manuscript. All authors read and approved the final manuscript.

Funding Open access funding provided by Uppsala University. This work was funded by the Swedish Research Council (Grant numbers [2018–05513], [2018–04524], and [2023–03788]) and the Knut and Alice Wallenberg Foundation (Grant number [KAW 2018.0191]).

Data availability The datasets generated during the current study are available in the figshare repository, under the DOI https://doi.org/10.6084/m9.figshare.24441430.

Declarations

Competing interests The authors have no relevant financial or non-financial interests to disclose.

Open Access This article is licensed under a Creative Commons Attribution 4.0 International License, which permits use, sharing, adaptation, distribution and reproduction in any medium or format, as long as you give appropriate credit to the original author(s) and the source, provide a link to the Creative Commons licence, and indicate if changes were made. The images or other third party material in this article are included in the article's Creative Commons licence, unless indicated otherwise in a credit line to the material. If material is not included in the article's Creative Commons licence and your intended use is not permitted by statutory regulation or exceeds the permitted use, you will need to obtain permission directly from the copyright holder. To view a copy of this licence, visit http://creativecommons.org/licenses/by/4.0/.

References

Amon RMW, Benner R (1994) Rapid cycling of high-molecular-weight dissolved organic matter in the ocean. Nature 369:549–552. https://doi.org/10.1038/369549a0

Amon RMW, Benner R (1996) Bacterial utilization of different size classes of dissolved organic matter. Limnol Oceanogr 41:41–51. https://doi.org/10.4319/lo.1996.41.1.0041

Andersson E, Meklesh V, Gentile L et al (2023) Generation and properties of organic colloids extracted by water from the organic horizon of a boreal forest soil. Geoderma 432:116386. https://doi.org/10.1016/j.geoderma.2023.116386

Andersson E, Meklesh V, Gentile L et al (2023) A contrast variation SANS and SAXS study of soil derived dissolved organic matter, and its interactions with hematite nanoparticles. JCIS Open 11:100091. https://doi.org/10.1016/j.jciso.2023.100091

Andreasson F, Bergkvist B, Bååth E (2009) Bioavailability of DOC in leachates, soil matrix solutions and soil water extracts from beech forest floors. Soil Biol Biochem 41:1652–1658. https://doi.org/10.1016/j.soilbio.2009.05.005

Attermeyer K, Catalán N, Einarsdottir K et al (2018) Organic carbon processing during transport through boreal inland waters: particles as important sites. J Geophys Res Biogeosci 123:2412–2428. https://doi.org/10.1029/2018JG004500

Berggren M, Guillemette F, Bieroza M et al (2022) Unified understanding of intrinsic and extrinsic controls of dissolved organic carbon reactivity in aquatic ecosystems. Ecology. https://doi.org/10.1002/ecy.3763

Bolan NS, Adriano DC, Kunhikrishnan A et al (2011) Dissolved organic matter: biogeochemistry, dynamics, and environmental significance in soils. In: Sparks DL (ed) Advances in agronomy. Academic Press, San Diego, pp 1–75

Bowen SR, Gregorich EG, Hopkins DW (2009) Biochemical properties and biodegradation of dissolved organic matter from soils. Biol Fertil Soils 45:733–742. https://doi.org/10.1007/s00374-009-0387-6

Catalá TS, Shorte S, Dittmar T (2021) Marine dissolved organic matter: a vast and unexplored molecular space. Appl Microbiol Biotechnol 105:7225–7239. https://doi.org/10.1007/s00253-021-11489-3

Cleveland CC, Neff JC, Townsend AR, Hood E (2004) Composition, dynamics, and fate of leached dissolved organic matter in terrestrial ecosystems: results from a decomposition experiment. Ecosystems. https://doi.org/10.1007/s10021-003-0236-7

Davidson EA, Galloway LF, Strand MK (1987) Assessing available carbon: comparison of techniques across selected forest soils. Commun Soil Sci Plant Anal 18:45–64. https://doi.org/10.1080/00103628709367802

Don A, Kalbitz K (2005) Amounts and degradability of dissolved organic carbon from foliar litter at different decomposition stages. Soil Biol Biochem 37:2171–2179. https://doi.org/10.1016/j.soilbio.2005.03.019

Dreves A, Andersen N, Grootes PM et al (2007) Colloidal matter in water extracts from forest soils. Environ Chem 4:424. https://doi.org/10.1071/EN07057

Evans DF, Wennerström H (1999) The colloidal domain: where physics, chemistry, biology, and technology meet, 2nd edn. Wiley-VCH, New York

Fernández C, Wider G (2006) NMR spectroscopy of large biological macromolecules in solution. In: Arrondo JLR, Alonso A (eds) Advanced techniques in biophysics. Springer, Berlin, pp 89–128

Findlay SEG, Parr TB (2017) Dissolved organic matter. In: Lamberti GA, Hauer FR (eds) Methods in stream ecology, 3rd edn. Academic Press, San Diego, pp 21–36

Gentile L, Wang T, Tunlid A et al (2018) Ferrihydrite nanoparticle aggregation induced by dissolved organic matter. J Phys Chem A 122:7730–7738. https://doi.org/10.1021/acs.jpca.8b05622

Gentile L, Floudas D, Olsson U et al (2024) Fungal decomposition and transformation of molecular and colloidal fractions of dissolved organic matter extracted from boreal forest soil. Soil Biol Biochem 195:109473. https://doi.org/10.1016/j.soilbio.2024.109473

Glatter O (2018) Scattering methods and their application in colloid and interface science. Elsevier, Amsterdam

Grasset C, Groeneveld M, Tranvik LJ et al (2023) Hydrophilic species are the most biodegradable components of freshwater dissolved organic matter. Environ Sci Technol 57:13463–13472. https://doi.org/10.1021/acs.est.3c02175

Herbert BE, Bertsch PM (1995) Characterization of dissolved and colloidal organic matter in soil solution: a review. In: McFee WW, Kelly JM (eds) Carbon forms and functions in forest soils. Soil Science Society of America, Madison, pp 63–88

Hwang TL, Shaka AJ (1995) Water suppression that works. excitation sculpting using arbitrary wave-forms and pulsed-field gradients. J Magn Reson A 112:275–279. https://doi.org/10.1006/jmra.1995.1047

Kalbitz K, Schmerwitz J, Schwesig D, Matzner E (2003) Biodegradation of soil-derived dissolved organic matter as related to its properties. Geoderma 113:273–291. https://doi.org/10.1016/S0016-7061(02)00365-8

Kalbitz K, Schwesig D, Schmerwitz J et al (2003) Changes in properties of soil-derived dissolved organic matter induced by biodegradation. Soil Biol Biochem 35:1129–1142. https://doi.org/10.1016/S0038-0717(03)00165-2

Kalbitz K, Schwesig D, Rethemeyer J, Matzner E (2005) Stabilization of dissolved organic matter by sorption to the mineral soil. Soil Biol Biochem 37:1319–1331. https://doi.org/10.1016/j.soilbio.2004.11.028

Kellerman AM, Kothawala DN, Dittmar T, Tranvik LJ (2015) Persistence of dissolved organic matter in lakes related to its molecular characteristics. Nature Geosci 8:454–457. https://doi.org/10.1038/ngeo2440

Kepkay PE (1994) Particle aggregation and the biological reactivity of colloids. Mar Ecol Prog Ser. https://doi.org/10.3354/meps109293

Kepkay PE, Johnson BD (1989) Coagulation on bubbles allows microbial respiration of oceanic dissolved organic carbon. Nature 338:63–65. https://doi.org/10.1038/338063a0

Kiikkilä O, Kitunen V, Smolander A (2006) Dissolved soil organic matter from surface organic horizons under birch and conifers: degradation in relation to chemical characteristics. Soil Biol Biochem 38:737–746. https://doi.org/10.1016/j.soilbio.2005.06.024

Kleber M, Eusterhues K, Keiluweit M et al (2015) Mineral-organic associations: formation, properties, and relevance in soil environments. In: Sparks DL (ed) Advances in agronomy. Academic Press, San Diego, pp 1–140

Koehler B, von Wachenfeldt E, Kothawala D, Tranvik LJ (2012) Reactivity continuum of dissolved organic carbon decomposition in lake water. J Geophys Res Biogeosci. https://doi.org/10.1029/2011JG001793

Kothawala DN, Kellerman AM, Catalán N, Tranvik LJ (2021) Organic matter degradation across ecosystem boundaries: the need for a unified conceptualization. Trends Ecol Evol 36:113–122. https://doi.org/10.1016/j.tree.2020.10.006

Lehmann J, Kleber M (2015) The contentious nature of soil organic matter. Nature 528:60–68. https://doi.org/10.1038/nature16069

Lehmann K, Lehmann R, Totsche KU (2021) Event-driven dynamics of the total mobile inventory in undisturbed soil account for significant fluxes of particulate organic carbon. Sci Total Environ 756:143774. https://doi.org/10.1016/j.scitotenv.2020.143774

Liu F, Wang D, Zhang B, Huang J (2021) Concentration and biodegradability of dissolved organic carbon derived from soils: a global perspective. Sci Total Environ 754:142378. https://doi.org/10.1016/j.scitotenv.2020.142378

Marschner B, Kalbitz K (2003) Controls of bioavailability and biodegradability of dissolved organic matter in soils. Geoderma 113:211–235. https://doi.org/10.1016/S0016-7061(02)00362-2

Meklesh V, Gentile L, Andersson E et al (2022) Characterization of the colloidal properties of dissolved organic matter from forest soils. Front Soil Sci 2:832706. https://doi.org/10.3389/fsoil.2022.832706

Mueller CW, Schlund S, Prietzel J et al (2012) Soil aggregate destruction by ultrasonication increases soil organic matter mineralization and mobility. Soil Sci Soc Am J 76:1634–1643. https://doi.org/10.2136/sssaj2011.0186

Nebbioso A, Piccolo A (2013) Molecular characterization of dissolved organic matter (DOM): a critical review. Anal Bioanal Chem 405:109–124. https://doi.org/10.1007/s00216-012-6363-2

Olsson U, Soederman O, Guering P (1986) Characterization of micellar aggregates in viscoelastic surfactant solutions. a nuclear magnetic resonance and light scattering study. J Phys Chem 90:5223–5232. https://doi.org/10.1021/j100412a066

Qualls RG, Haines BL (1992) Biodegradability of dissolved organic matter in forest throughfall, soil solution, and stream water. Soil Sci Soc Am J 56:578–586. https://doi.org/10.2136/sssaj1992.03615995005600020038x

Schlesinger WH (2020) Biogeochemistry: an analysis of global change, 4th edn. Elsevier, SanDiego

Schmidt MWI, Torn MS, Abiven S et al (2011) Persistence of soil organic matter as an ecosystem property. Nature 478:49–56. https://doi.org/10.1038/nature10386

Škerlep M, Nehzati S, Johansson U et al (2022) Spruce forest afforestation leading to increased Fe mobilization from soils. Biogeochemistry 157:273–290. https://doi.org/10.1007/s10533-021-00874-9

Søndergaard M, Middelboe M (1995) A cross-system analysis of labile dissolved organic carbon. Mar Ecol Prog Ser 118:283–294. https://doi.org/10.3354/meps118283

Sundman A, Karlsson T, Laudon H, Persson P (2014) XAS study of iron speciation in soils and waters from a boreal catchment. Chem Geol 364:93–102. https://doi.org/10.1016/j.chemgeo.2013.11.023

Tranvik LJ (1990) Bacterioplankton growth on fractions of dissolved organic carbon of different molecular weights from humic and clear waters. Appl Environ Microbiol 56:1672–1677. https://doi.org/10.1128/aem.56.6.1672-1677.1990

Ulmius J, Wennerström H (1977) Proton NMR bandshapes for large aggregates; micellar solutions of hexadecyltrimethylammonium bromide. J Magn Reson 28:309–312. https://doi.org/10.1016/0022-2364(77)90161-5

Wennerström H, Ulmius J (1976) Proton NMR bandshapes in phospholipid bilayer vesicles. J Magn Reson 23:431–435. https://doi.org/10.1016/0022-2364(76)90276-6

Whitty SD, Waggoner DC, Cory RM et al (2019) Direct noninvasive 1 H NMR analysis of stream water DOM: insights into the effects of lyophilization compared with whole water. Magn Reson Chem. https://doi.org/10.1002/mrc.4935

Yan J, Manelski R, Vasilas B, Jin Y (2018) Mobile colloidal organic carbon: an underestimated carbon pool in global carbon cycles? Front Environ Sci 6:148. https://doi.org/10.3389/fenvs.2018.00148

Publisher's Note Springer Nature remains neutral with regard to jurisdictional claims in published maps and institutional affiliations.